Nonlinear Robust Vibration Control of a Plate Integrated with Piezoelectric Actuator

A. Oveisi and M. Gudarzi

***Abstract*—**This paper investigates the vibration control of a nonlinear plate using piezoelectric actuator based on an adaptive robust control algorithm. A complete mathematical modeling is presented in order to describe the dynamic of plate motion. Then, a robust adaptive fuzzy control algorithm, for controlling the proposed mechanical structure, is introduced. This controller includes a fuzzy scheme and a robust controller. Based on sliding mode controller a fuzzy system is introduced to mimic an ideal controller. The robust controller is designed based on compensation of the difference between the fuzzy controller and the ideal controller. The parameters of the fuzzy system and uncertainty bound of the robust controller are adjusted adaptively. The adaptive laws are designed based on the Lyapunov stability theorem to reach the stability of the closed-loop system. Detailed analysis for the closed-loop system is carried out to evaluate the vibration controller performance due to output excitation. Finally, the effect of initial condition on vibration characteristic is investigated, numerically.

***Keywords*—**Smart structure, nonlinear vibration, piezoelectric, strain gauge sensor.

I. Introduction

In recent years, the light plates have been widely used in mechanical, aeronautical and civil structures, because of their requirements to become lighter, more flexible and stronger. By studying the works in the field of the vibrations of elastic plates, such as those by Kung and Pao [1], Kisliakov [2] and Pasic and Herrmann [3] one can easily see that most of them are concerned with problems in which only one spatial mode is strongly excited. However, Sridhar, Mook and Nayfeh [4, 5] and Yang and Sethna [6] represented the motion with higher order mode to consider the effect of internal resonance and the modal interactions. In references [4, 5] the natural frequencies assure special relationships, while in reference [6] the equations are evaluated by the averaging procedure.

From control view of point, smart materials have been used to develop operational quality or reduce the noise amplitude of the structures under vibratory excitation in a wide range. Control strategy plays a crucial role in these structures, especially in the lightweight ones. So, many researchers have been interested in designing appropriate controllers for smart materials with practical geometries [7]. The Positive Position Feedback (PPF) controller is used by Shan *et al.* for a flexible structure [8]. They compared the results with the algorithm of velocity feedback. Kwak and Heo investigated the effect of the PPF algorithm on the model of a solar panel [9]. Gudarzi *et al.* have implemented a linear robust control approach on a piezolaminated thin plate. Also, μ analysis has been taken in to account to ensure the robust performance of the uncertain system in wide range of frequencies [10]. Oueini *et al.* have studied a nonlinear controller based on saturation phenomena working as a vibration absorber for a linear model of a cantilever beam [11]. They inspected different parameters influence such as loops gains, damping of the controller and the initial condition on the performance of the closed-loop system. Pai *et al.* compared two control approaches of linear position feedback algorithm and the Nonlinear Saturation Control (NSC) in an experimental test [12]. They demonstrated the advantages of hybrid, proportional linear and saturation nonlinear controller. Saguranrum *et al.* showed the influence of non-uniformities in the structure properties for a beam with the saturation controller [13]. The reason of these non-uniformities is the imperfect bounding of the piezo-actuator on the host layer. Hashemi-dehkordi *et al.*, by applying an intelligent Active Force Control (AFC) based method, introduced a new approach to reduce the effect of negative damping that leads to Friction Induced Vibration [14]. Also, the effectiveness of the PID-AFC method in comparison with PID is investigated both in time domain and frequency domain. Karaarslan employed piezoceramic as a single phase Sheppard-Taylor converter to present a harvesting vibrational energy system [15]. The energy is gained using the piezoceramics and the converter controls the power flow to the preferred load. Oueini and Nayfeh introduce the algorithm of cubic velocity feedback for the first time in controlling of a nonlinear vertically excited beam [16]. They analyzed analytical bifurcation in the simulation and experimental results. Sodano *et al.* used Macro Fiber Composite (MFC) self-sensing actuators for vibration attenuation of inflated torus [17]. They presented the advantages of this kind of actuator in comparison with traditional PZT elements. Jun *et al.* implemented NSC for a nonlinear system by applying PZT patches [18].

In the last few years, the research on controlling chaos has attracted a wide range of attention from engineering, physics, mathematics, and biology. The development of this field is started by Ott *et al.* [19]. They first introduced a new method for controlling a nonlinear dynamical structural system.

A. Oveisi is with the Iran University of Science and Technology, Narmak, Tehran, Iran, 1684613114 (e-mail: atta.oveisi@gmail.com).

M. Gudarzi is with the Mechanical Engineering Department, Damavand Branch, Islamic Azad University, Damavand, Tehran, Iran (corresponding author to provide phone: 98-912-7021043; e-mail: mohammad.gudarzi@gmail.com).

Numerous control methods have been proposed for controlling chaos [20-23] after that. Several nonlinear control techniques, such as feedback linearization [24], sliding-mode control [25-27], backstepping [28,29], and adaptive control algorithms [30,31] have been also applied for controlling of chaotic systems.

Recently, fuzzy logic control (FLC) has involved attention in control problems [32-38]. FLC systems offer an effective advance to handle nonlinear systems, especially in the presence of uncertainty of the plant or the situation where precise control action is unavailable. Different FLC schemes have been proposed for nonlinear and uncertain systems based on fuzzy systems. However, the main drawback of FLC systems is the lack of a systematic control design methodology. Particularly, stability analysis of an FLC system due to their nonlinearity is generally a long procedure [39].

In this paper, the application of a robust adaptive fuzzy control scheme to the case of nonlinear composite plate vibration is proposed. The dynamic model of the plate is based that is given by Chu and Herrmann [40] which is the dynamic analogue of the von Karman partial differential equations of the plate. The controller comprises a fuzzy system and a robust controller. The fuzzy system, with online tuned parameters is designed based on the, ideal, sliding-mode control (SMC). The robust controller is implemented to recompense for the divergence between the fuzzy and the ideal controllers. The uncertainty bound needed in the robust controller is also adaptively tuned online to avoid unnecessary high gain resulted from using fixed and most often conservative bounds. The adaptive laws are derived in the Lyapunov sense, thus, the asymptotic stability of the controlled system is guaranteed. Analysis of the control strategy for a strongly nonlinear plant and high level of amplitude of excitation is a contribution of this study. Piezo-actuators are used for the real implementation of the control strategy, which allows achieving the required vibration level.

II. Dynamic Modeling of the Plate

Consider a flat square plate of thickness h and edge length a. All of the edges are simply supported. The plate is subjected to a lateral excitation force normal to the plate and a constant in-plane stress along the edges. A sketch of the system being studied is shown in Fig. 1.

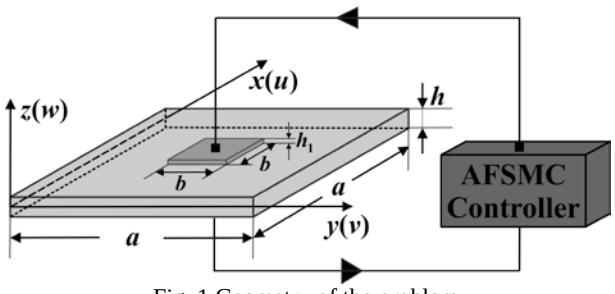

Fig. 1 Geometry of the problem

The governing equations of an isotropic plate derived by Chu and Herrmann [40] are

$$\begin{aligned}
&u^0_{xx} + d_1 u^0_{yy} + d_2 v^0_{xy} \\
&\qquad = -w^0_x\left(w^0_{xx} + d_1 w^0_{yy}\right) - d_2 w^0_y w^0_{xy}, \\
&v^0_{yy} + d_1 v^0_{xx} + d_2 u^0_{xy} \\
&\qquad = -w^0_y\left(w^0_{yy} + d_1 w^0_{xx}\right) - d_2 w^0_x w^0_{xy}, \\
&D\nabla^4_{xy} w^0 + \rho h w^0_{tt} + 2c w^0_t \\
&\qquad = q^0 \\
&\qquad + \frac{Eh}{1-\nu^2}\left[\left(u^0_x + \frac{1}{2}(w^0_x)^2\right)\left(w^0_{xx}\right.\right. \\
&\qquad \left. + \nu w^0_{yy}\right) \\
&\qquad + \left(v^0_y + \frac{1}{2}\left(w^0_y\right)^2\right)\left(w^0_{yy} + \nu w^0_{xx}\right) \\
&\qquad \left. + (1-\nu) w^0_{xy}\left(u^0_y + v^0_x + w^0_x w^0_y\right)\right], \\
&\nabla^4_{xy} W^0 = w^0_{xxxx} + 2w^0_{xxyy} + w^0_{yyyy},
\end{aligned} \tag{1}$$

where

$$d_1 = \frac{1-\nu}{2}, \qquad d_2 = \frac{1+\nu}{2}, \qquad D = \frac{Eh^2}{12(1-\nu^2)},$$

and the membrane forces are

$$N_x = \frac{Eh}{1-\nu^2}\left[u^0_x + \nu v^0_y + \frac{1}{2}\left((w^0_x)^2 + \nu\left(w^0_y\right)^2\right)\right],$$

$$N_y = \frac{Eh}{1-\nu^2}\left[v^0_y + \nu u^0_x + \frac{1}{2}\left(\left(w^0_y\right)^2 + \nu(w^0_x)^2\right)\right],$$

where u^0 and v^0 are the displacements in the mid-plane of the plate in the x- and y- directions respectively, w^0 is the displacement in the plane normal to the mid-plane and E, ν and ρ are the modulus of elasticity, the Poisson ratio and the density, respectively. Also, c is the coefficient of lateral viscous damping and q^0 is the lateral excitation.

We express the governing equations and the membrane forces in the non-dimensional form

$$\begin{aligned}
&u_{\zeta\zeta} + d_1 u_{\eta\eta} + d_2 v_{\zeta\eta} \\
&\qquad = -w_\zeta\left(w_{\zeta\zeta} + d_1 w_{\eta\eta}\right) - d_2 w_\eta w_{\zeta\eta},
\end{aligned} \tag{2a}$$

$$\begin{aligned}
&v_{\eta\eta} + d_1 v_{\zeta\zeta} + d_2 u_{\zeta\eta} \\
&\qquad = -w_\eta\left(w_{\eta\eta} + d_1 w_{\zeta\zeta}\right) - d_2 w_\zeta w_{\zeta\eta},
\end{aligned} \tag{2b}$$

$$\begin{aligned}
&\nabla^4_{\zeta y} w + 4\Omega^2 w_{\tau\tau} + 2\Omega\mu w_\tau \\
&\qquad = q \\
&\qquad + 12\left[\left(u_\zeta + \frac{1}{2}\left(w_\zeta\right)^2\right)\left(w_{\zeta\zeta} + \nu w_{\eta\eta}\right)\right. \\
&\qquad + \left(v_\eta + \frac{1}{2}\left(w_\eta\right)^2\right)\left(w_{\eta\eta} + \nu w_{\zeta\zeta}\right) \\
&\qquad \left. + (1-\nu) w_{\zeta\eta}\left(u_\eta + v_\zeta + w_\zeta w_\eta\right)\right],
\end{aligned} \tag{2c}$$

$$\begin{aligned}
&N_\zeta = \frac{\pi^2 Eh^3}{(1-\nu^2)a^2}\left[u^0_\zeta + \nu v^0_\eta + \frac{1}{2}\left(\left(w^0_\zeta\right)^2 + \nu\left(w^0_\eta\right)^2\right)\right], \\
&N_\eta = \frac{\pi^2 Eh^3}{(1-\nu^2)a^2}\left[v^0_\eta + \nu u^0_\zeta + \frac{1}{2}\left(\left(w^0_\eta\right)^2 + \nu\left(w^0_\zeta\right)^2\right)\right],
\end{aligned} \tag{3}$$

with

$$\zeta = \frac{\pi x}{a}, \qquad \eta = \frac{\pi y}{a}, \qquad \tau = \omega t,$$

where

$$u^0 = \frac{\pi h^2 u}{a}, \qquad v^0 = \frac{\pi h^2 v}{a}, \qquad w^0 = hw,$$

$$\omega_0^2 = \frac{\pi^4 E h^2}{3\rho(1-\nu^2)a^4}, \qquad \Omega = \frac{\omega}{\omega_0}, \qquad \mu = \frac{4c}{\rho h \omega_0},$$
$$q = \frac{12(1-\nu^2)q^0 a^4}{\pi^4 E h^4},$$

We further assume that the lateral load is distributed symmetrically and sinusoidal so that the related spatial modes are effectively excited. Considering these, one can choose the first two fundamental orthogonal mode shapes to capture the motion and study their interaction. Thus, a solution of w in equations (2) is assumed to be

$$w = z_1 \sin\zeta \sin\eta + z_2 \sin 3\zeta \sin\eta, \qquad z_1 = z_1(\tau), \qquad z_2 = z_2(\tau), \tag{4}$$

where z_1 and z_2 are the amplitudes of the modes and ζ and η are from 0 to π. Substituting equation (4) into equation (2a, b), u and v can be computed with the aid of a symbolic computational tool, to give

$$u = A_1 \sin 2\zeta + A_2 \sin 2\zeta \cos 2\eta + A_3 \sin 4\zeta + A_4 \sin 4\zeta \cos 2\eta + A_5 \sin 6\zeta + A_6 \sin 6\zeta \cos 2\eta, \tag{5}$$
$$v = A_7 \sin 2\eta + A_8 \cos 2\zeta \sin 2\eta + A_9 \cos 4\zeta \sin 2\eta + A_{10} \cos 6\zeta \sin 2\eta,$$

where A_i are the polynomials of z_1 and z_2 listed below

$$A_1 = \frac{z_1\{(\nu-1)z_1 - (6+2\nu)z_2\}}{16}, \qquad A_2 = \frac{z_1(4z_1 + 16z_2 + 8\nu z_2)}{64},$$
$$A_3 = \frac{(-3+\nu)z_1 z_2}{16}, \qquad A_4 = \frac{(19-\nu)z_1 z_2}{100},$$
$$A_5 = \frac{(-9+\nu)z_2^2}{48}, \qquad A_6 = \frac{3z_2^2}{16}, \tag{6}$$
$$A_7 = \frac{-z_1^2 + \nu z_1^2 - z_2^2 + 9\nu z_2^2}{16}, \qquad A_8 = \frac{z_1(4z_1 - 16z_2 + 8\nu z_2)}{64},$$
$$A_9 = \frac{(29-\nu)z_1 z_2}{200}, \qquad A_{10} = \frac{z_2^2}{16},$$

If constant in-plane stresses N_x and N_y are taken into account, the displacement functions u and v should be modified to be $u \to B\zeta + u,\ v \to C\eta + v$ [10]. Where B and C are constants to be determined by equation (3) with modified u and v in equation (6) and assumed w in equation (4). Thus one will have

$$B = \frac{a^2}{\pi^2 E h^3}(N_x - \nu N_y), \qquad C = \frac{a^2}{\pi^2 E h^3}(N_y - \nu N_x), \tag{7}$$

By substituting the displacement functions given in equations (4) and (6) into equation (2c) and using the Galerkin method, two coupled nonlinear second order ordinary differential equations of independent variable τ are obtained, as

$$4\Omega^2 \ddot{z}_1 + 2\Omega\mu\dot{z}_1 + k_1 z_1 + \alpha_{11} z_1^3 + \alpha_{12} z_1 z_2^2 + \alpha_{13} z_2 z_1^2 = q_1(\tau),$$
$$4\Omega^2 \ddot{z}_2 + 2\Omega\mu\dot{z}_2 + k_2 z_2 + \alpha_{21} z_2^3 + \alpha_{22} z_2 z_1^2 + \alpha_{23} z_1^3 = q_2(\tau), \tag{8}$$

where k_i and α_{ij} are given as [41].

$$k_1 = 4 + \frac{12(1-\nu^2)a^2}{\pi^2 E h^3}(N_x + N_y),$$
$$\alpha_{11} = \frac{9}{4} + \frac{3\nu}{4} - \frac{3\nu^2}{2},$$
$$\alpha_{12} = \frac{753}{100} - \frac{21\nu}{4} - \frac{630\nu^2}{50},$$
$$\alpha_{13} = -\frac{45(1-\nu)}{8} + \frac{9\nu^2}{4},$$
$$k_2 = 100 + \frac{12(1-\nu^2)a^2}{\pi^2 E h^3}(9N_x + N_y),$$
$$\alpha_{21} = \frac{369}{4} + \frac{27\nu}{4} - \frac{123\nu^2}{2},$$
$$\alpha_{22} = \frac{753}{100} + \frac{51\nu}{4} - \frac{639\nu^2}{50},$$
$$\alpha_{23} = -\frac{3}{2} - \frac{3\nu}{4} + \frac{3\nu^2}{4},$$

and $q_1(\tau)$ and $q_2(\tau)$ are the amplitudes of the mode $\sin\zeta \sin\eta$ and the mode $\sin 3\zeta \sin\eta$ of the lateral excitation q respectively.

III. Controller Design

Sliding-mode control, based on the theory of variable structure systems, has been widely used to robust control of nonlinear systems. Sliding mode controllers act in presence of uncertainty and disturbances and cause the closed-loop system be robust stable with consistency of performance [42, 43]. In general, the design of SMCs consists of two steps: The first step is finding a feedback controller which causes the state trajectory to reach the sliding surface s in finite time and thereafter remain on s, and the second is to guarantee that the resulting trajectory on s is stable. Consider the following n-th order chaotic dynamic system,

$$x^{(n)} = f(x) + g(x)u, \tag{9}$$

where $x = [x\ \dot{x}\ \ \ldots\ \ x^{n-1}] = [x_1\ x_2 \ldots x_n] \in R^n$ is the vector of states which are assumed to be measurable, $u \in R$ is the control input, $f(x)$ and $g(x)$ are smooth functions which are not known a priori. The tracking error is defined as

$$\tilde{x}(t) = x_d(t) - x(t), \tag{10}$$

where $x_d(t)$ represents the desired trajectory. The objective is to determine a controller for the system described by (9), so that the tracking error converges to zero while maintaining all signals bounded.

In the presence of uncertainties, the chaotic system (9) is modified as

$$x^{(n)} = [f_n(x) + \Delta f(x)] + [g_n(x) + \Delta g(x)]u, \tag{11}$$

In which f_n and g_n are the nominal values, and $\Delta f(x)$ and $\Delta g(x)$ are the uncertainties of f and g, respectively. (11) can be rewritten as

$$x^{(n)} = f(x) + g(x)u + d, \tag{12}$$

where d is the lumped uncertainty, defined as $d = f(x) + g(x)u$. It is assumed that the lumped uncertainty is bounded such that $|d| \le \delta$. Let the time derivative operator be $D \triangleq d/dt$, and define a sliding surface as

$$s = (D + \lambda)^{n-1}\tilde{x}, \tag{13}$$

With $\lambda > 0$ a user defined constant. The time derivative of s can be obtained as

$$\dot{s} = D(D+\lambda)^{n-1}\tilde{x} = \left(D^n + \sum_{i=1}^{n-1} C_i^{n-1} D^{n-i}\lambda^i\right)\tilde{x} \quad (14)$$

where $C_r^n = \left(\frac{n!}{r!(n-r)!}\right)$. The sliding-mode control law is defined as $u = u_{eq} + u_{rb}$. Where the equivalent controller u_{eq} is a feedback linearization controller, obtained from $\dot{s} = 0$,

$$u_{eq} = g^{-1}(x)\left[-f(x) + x_n^{(n)} + \sum_{i=1}^{n-1} C_i^{n-1} D^{n-i}\lambda^i\tilde{x}\right], \quad (15)$$

and the robust controller u_{rb} is designed to dispel the uncertainties as

$$u_{rb} = g^{-1}[\delta\ \mathrm{sgn}(s)] \quad (16)$$

Substituting (15), (16) into (12), and using (14) yields

$$-d - \delta\ \mathrm{sgn}(s) = x_d^{(n)} - x^n + \sum_{i=1}^{n-1} C_i^{n-1} D^{n-i}\lambda^i\tilde{x} = \dot{s}, \quad (17)$$

Then consider the following candidate Lyapunov function $V_1 = \frac{1}{2}s^2$, differentiating the Lyapunov function with respect to time and using (17) yields

$$\begin{aligned}\dot{V}_1 = s\dot{s} &= -sd - |s|\delta \le |s||d| - |s|\delta \\ &= -|s|(\delta - |d|) \le 0\end{aligned} \quad (18)$$

Therefore, the SMC system introduced by $u = u_{eq} + u_{rb}$ can guarantee the stability of the uncertain system (12) in the Lyapunov sense. In the design of the SMC, the uncertainty bound d, which includes unknown dynamics, parameter variations, and external load disturbance, must be available. However, the bound of uncertainties is difficult to obtain in advance for practical applications. Moreover, to satisfy the existence condition of the sliding-mode, a conservative control law with large control effort usually results by using fixed, and most often conservative, bounds [44]. In order to exploit the advantages, and tackle the disadvantages, of both SMC and FLC systems, a hybrid control scheme is proposed in this study, referred to as adaptive fuzzy sliding-mode control (AFSMC) system. This approach provides a systematic way to design FLC systems while retaining the robustness and asymptotic stability properties of SMC.

Assume that the parameters of the system (37) are well known. Then an ideal controller can be obtained as

$$u^* = g^{-1}(x)\left[-f(x) + x_d^{(n)} + \sum_{i=1}^{n-1} C_i^{n-1} D^{n-i}\lambda^i\tilde{x}\right], \quad (19)$$

By substituting (19) in (9) the resulting error dynamic is

$$\left(D^n + \sum_{i=1}^{n-1} C_i^{n-1} D^{n-i}\lambda^i\right)\tilde{x} = 0, \quad (20)$$

By proper selection of λ as the coefficients of a Hurwitz polynomial, the error dynamic is stable. However, since the system is not known completely, the ideal controller u^* cannot be implemented precisely, therefore, as an alternative, using the universal approximation capability of fuzzy systems, the ideal controller can be approximated by a fuzzy system.

Consider an n_i-input, single-output fuzzy system with n_r fuzzy IF-THEN rules as

Rule r: If x_1 is $\tilde{A}_1^r$ and … and x_{n_i} is $\tilde{A}_{n_i}^r$ then $y = \tilde{b}^r$

where $x = [x_1 \dots x_{n_i}]$ and y are the input and output of the fuzzy system, respectively, $\tilde{b}^r$ is the fuzzy singleton for the output of the rth rule, and $\tilde{A}_1^r \dots \tilde{A}_{n_i}^r$ are fuzzy sets characterized by Gaussian membership functions as

$$\mu_{A_j^r}(x_j) = exp\left[-\left(\frac{x_j - c_j^r}{\sigma_j^r}\right)\right], \quad (21)$$

In which c_j^r and σ_j^r are the center and width of the Gaussian membership function. Using singleton fuzzifier, product inference, and center average defuzzifier, the output of the fuzzy system is obtained as

$$y = \frac{\sum_{r=1}^{n_r} \tilde{b}^r \prod_{j=1}^{n_i} \mu_{A_j^r}(x_j)}{\sum_{r=1}^{n_r} \prod_{i=1}^{n_i} \mu_{A_i^j}(x_i)}, \quad (22)$$

Define the firing strength of the r- th rule as

$$w^r = \frac{\prod_{j=1}^{n_i} \mu_{A_j^r}(x_j)}{\sum_{r=1}^{n_r} \prod_{i=1}^{n_i} \mu_{A_i^j}(x_i)}, \quad (23)$$

Then the output of the fuzzy system can be rewritten as

$$y = B^T W, \quad (24)$$

where $B = \left[\tilde{b}^1 \dots \tilde{b}^{n_r}\right]^T$ and $W = [w^1 \dots w^{n_r}]^T$. It has been proven that fuzzy system (24) is a universal approximator [39]. Therefore, the ideal controller (19) can be approximated by an ideal fuzzy system $u_{fuz}^*(s, B^*)$ such that

$$u^* = u_{fuz}^*(s, B^*) + \psi = \hat{B^*}^T W + \psi, \quad (25)$$

where ψ is the approximation error or the uncertainty which is assumed to be bounded as $|\psi| < \Psi$ and B^* is the optimal parameter vector

$$B^* \triangleq \arg\min_B\{|B^T W - u^*|\}, \quad (26)$$

The fuzzy IF–THEN rules of this fuzzy system have the following form

Rule r: If s is $\tilde{A}^r$ then $u_{fuz}^* = \tilde{b}^r$,

In practice, the optimal parameter vector B^*, as well as the uncertainty or approximation error bound Ψ may be unknown. Let $\hat{u}_{fuz}(s, \hat{B}) = \hat{B}^T W$ be a fuzzy system to approximate u^* as

$$u = \hat{u}_{fuz}(s, \hat{B}) + u_{rb}(s), \quad (27)$$

where the fuzzy controller $\hat{u}_{fuz}$ is designed to approximate the ideal controller u^*, and u_{rb} is designed to compensate for the difference between the ideal controller and fuzzy controller. Substitution of (27) into (1) yields

$$x^{(n)} = f(x) + g(x)\left[\hat{u}_{fuz}(s, \hat{B}) + u_{rb}(s)\right], \quad (28)$$

Multiplying (19) with $g(x)$, added to (28) and using (10) and (14), the error dynamic can be obtained as

$$\begin{aligned}&\left(D^n + \sum_{i=1}^{n-1} C_i^{n-1} D^{n-i}\lambda^i\right)\tilde{x} \\ &\qquad = g(x)\left[u^* - \hat{u}_{fuz} - u_{rb}(s)\right] = \dot{s},\end{aligned} \quad (29)$$

Defining the approximation errors as

$$\begin{aligned}\tilde{u}_{fuz} &= u^* - \hat{u}_{fuz}, \\ \tilde{B} &= B^* - \hat{B},\end{aligned} \quad (30)$$

and using (35) and (30) gives

$$\hat{u}_{fuz} = \tilde{B}^T W + \psi, \quad (31)$$

Moreover, denote the estimation of the uncertainty bound as Ψ

$$\tilde{\Psi}(t) = \Psi - \hat{\Psi}(t), \quad (32)$$

It can be proved that if the AFSMC system is designed as (27) in which the parameter vector of the fuzzy system is adaptively tuned according to

$$\dot{\hat{B}} = -\dot{\tilde{B}} = \alpha_1 s(t) W, \quad (33)$$

And the robust controller is designed as

$$u_{rb} = \hat{\Psi}\text{sgn}[s(t)]\text{sgn}(g), \quad (34)$$

With bound estimation algorithm given by

$$\dot{\hat{\Psi}} = -\dot{\tilde{\Psi}} = \alpha_2 |s(t)|\ \text{sgn}(g), \quad (35)$$

where α_1 and α_2 are positive constants known as learning rate, then the stability of the ASFMC is guaranteed.

IV. Numerical Example and Discussions

To examine the vibration behavior, we take a steel plate as an example. Since in the presented study we have only used two modes to represent the displacement w, a qualitative measure of the response is expected. More modes should be taken into account for quantitative results. The parameters of the plate are as follows: density $7850\ \text{kg/m}^3$, modulus of elasticity 200 GPa , Poisson ratio 0.3 coefficient of damping $\mu = 0.046$, length 1 m, thickness 0.01 m. We take the two boundary in-plane compressive stresses to be equal i.e. $N_x = N_y$, and of such value that k_1 equates say, 0.576. For the excitation we consider that $q_1 = f_1 \cos\tau$ and $q_2 = f_2 \cos\tau$ where f_i are force amplitudes. With the parameters

defined above, the equations (8) are rewritten as

$$4\Omega^2 \ddot{z}_1 + 2\Omega(0.046)\dot{z}_1 + 0.576\, z_1 + 2.34\, z_1^3 + 4.804\, z_1 z_2^2 - 3.735\, z_2 z_1^2 = f_1 \cos\tau,$$

$$4\Omega^2 \ddot{z}_2 + 2\Omega(0.046)\, \dot{z}_2 + 82.88\, z_2 + 88.74\, z_2^3 + 10.2048\, z_2 z_1^2 - 1.6575\, z_1^3 = f_2 \cos\tau,$$

The Piezo-patches have been chosen because of their suitable properties such as higher flexibility, durability and the electromechanical coupling constant. The schematic view of the smart plate is shown Fig. 2.

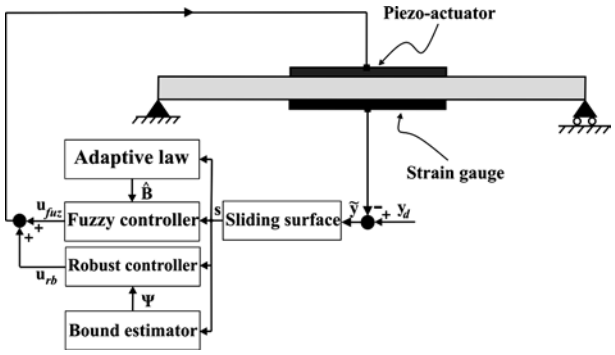

Fig. 2 Configuration of sensor/host/actuator

For flexible structures stiffening effect on the length of the actuator placement play a very important role [6]. Application of piezo-patches allows significant reduction of this effect and generation of larger deformations of the system. The response of the structure has been measured by a bounded-wire strain gauge, which has been mounted on the opposite side of the actuator side. The entire strain gauge is securely bonded to structural plate and will detect any deformation that may take place as shown in Fig. 3. Typically, the resistance change of a strain gauge is less than one ohm, so, measuring such small resistances usually requires a bridge circuit as that depicted in Fig. 3. Initially, the bridge is nulled by adjusting the resistances so that $V_1 = V_2$. The bridge also cancels out variations due to temperature changing, by connecting a dummy as one of the bridge resistors.

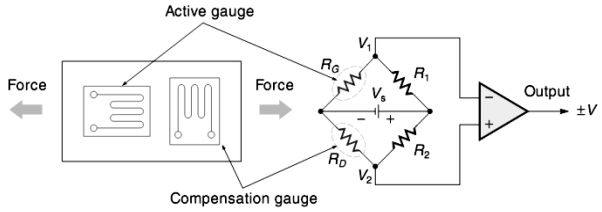

Fig. 3 Placement of the gauges and interface circuit using a bridge

By analyzing the bridge circuit of Fig. 3 as

$$V_1 = \frac{V_s R_G}{R_1 + R_G},$$

$$V_2 = \frac{V_s R_D}{R_2 + R_D},$$

The voltage across the bridge can be expressed as

$$\Delta V = V_s \frac{(R_G R_2 - R_D R_1)}{(R_1 + R_G)(R_2 + R_D)},$$

By simplifying the analysis, considering that all the resistors in the bridge have the same values R, we have

$$\Delta V = V_s \frac{\Delta R}{4R + 2\Delta R} \approx V_s \frac{\Delta R}{4R},$$

The input membership functions are selected as shown in Fig. 4.

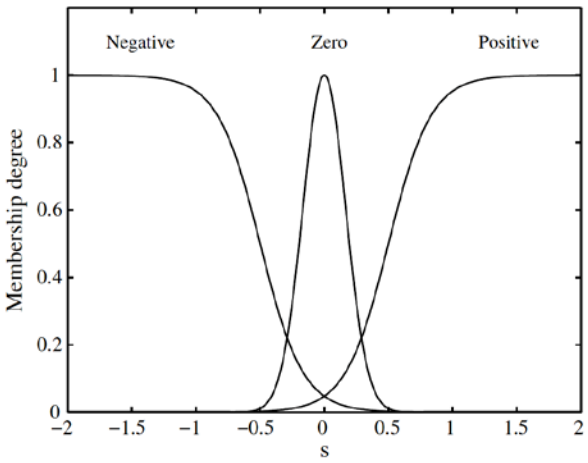

Fig. 4 Membership functions of s for AFSMC

The parameters of these membership functions are chosen such that the parameter s remains close to zero. The initial output membership functions are arbitrarily selected as $\hat{B} = [-1, 0, 1]^{\text{T}}$ and the initial value of uncertainty bound is chosen as $\Psi = 0.1$. The learning rates are set to $\alpha_1 = 10$ and $\alpha_2 = 1$. The actuator/sensor pair segments are assumed to be bounded on the top and the lower surface of the core layer and mechanical and electrical properties of piezo-actuator and

strain gauge are shown in TABLE I. In addition, the external load is considered a concentrated transverse harmonic load. For the design and simulation of the control system, MATLAB® Simulink were utilized, and a Multi-Input Single-Output (MISO) configuration, with the output being the voltage at the sensor location, and the input being the control voltage applied into the actuator of the top surface (see Fig. 2), was considered. In order to investigate the performance of controller in suppressing the vibration induced by harmonic external excitation, the displacement of the center point of the plate is shown in Fig. 5. It should be noted that the controller is forced to start after the time interval $[0 \quad 5]\ sec$ and the closed-loop performance can be evaluated after this time period.

TABLE I
MFC and strain gauge properties

Strain Gauge		Piezo-actuator	
Strain resistance	Gauge factor	Stack area	No-Load displacement at V_0 volts
100 Ohm	2	100 mm²	0.038
Initial deflection	Initial voltage	Test voltage V_0	Capacitance
0 mm	0 volts	120 volts	13 uF

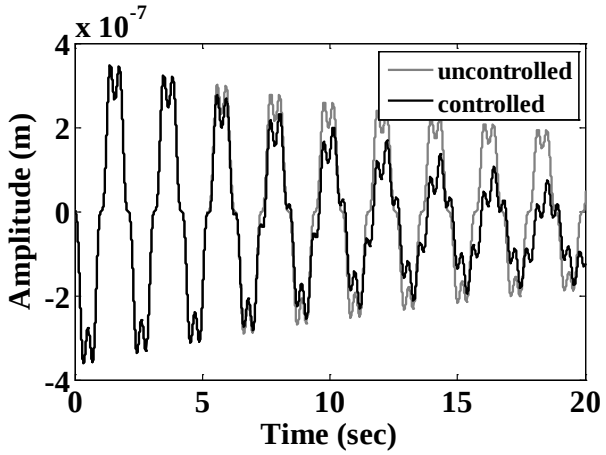

Fig. 5 Comparison of closed-loop and open loop displacement

This figure shows the comparison of the dynamic response of the open loop system and those obtained from closed-loop one by implementing robust AFSMC controller. It is clear that the nonlinear system vibrates with more than one harmony. However, in the closed-loop system, the displacement tends to reduce in amplitude oscillating with more harmonies and this is because of the nonlinearities that are added by controller. Also, the closed-loop system has done a great job in vibration attenuation. Because of consideration of the shear stress the displacement components in the x- and y- direction before and after implementing the controller is compared in Fig. 6.

Also, the control effort is depicted for the close-loop system as shown in Fig. 7. It can be seen that the control input does not have sudden jumps and can be applied in time domain. Also, as one can see, the control effort increases as time goes on and this is because of the fact that the compensator has to reduce the amplitude of vibration system under the harmonic excitation that acts on the plate continuously.

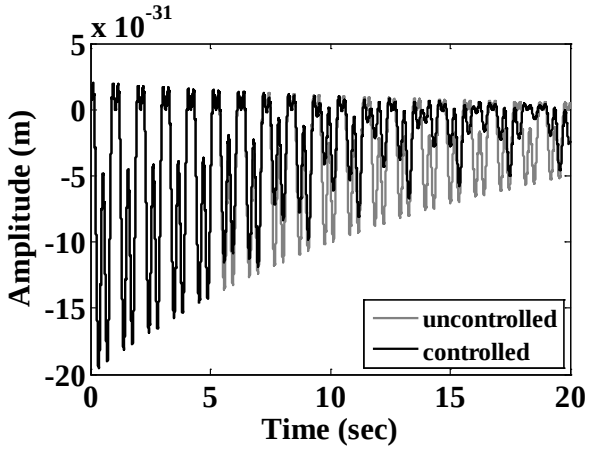

Fig. 6 Comparison of closed-loop and open loop displacement

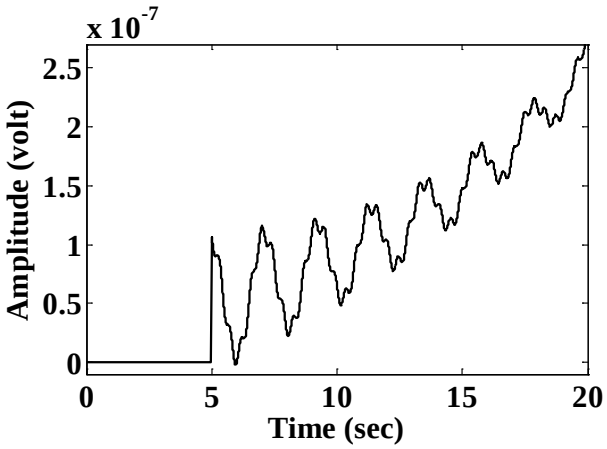

Fig. 7 Control effort

Figures 8 and 9 show the phase plane analysis for open loop system, closed-loop system using AFSMC compensator.

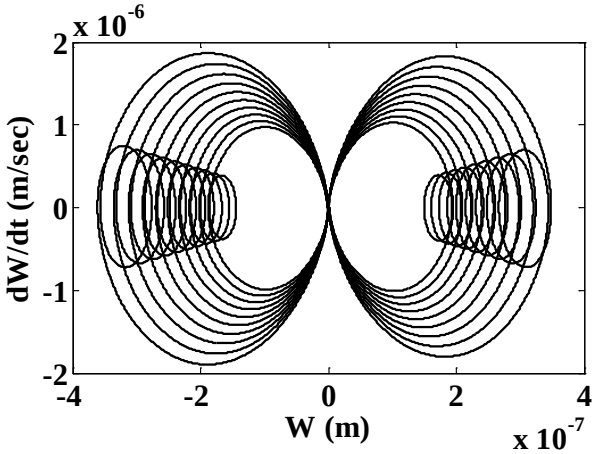

Fig. 8 Phase plane diagram of open loop system

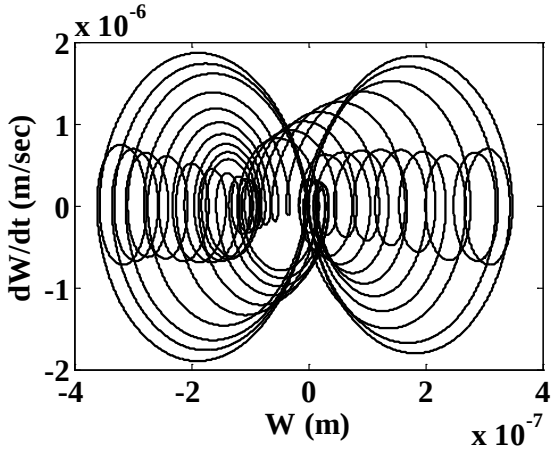

Fig. 9 Phase plane diagram of closed-loop system based on AFSMC controller

The main observations are as follows: the nonlinear behavior of the open loop and closed-loop system is a stable focus around the system equilibrium point and the whole state space. However, the closed-loop system damps the states to the equilibrium point faster. In addition, the intersection points in phase plane of non-autonomous systems do not sate for equilibrium points but occurs because of the nonlinearities and time dependency of the system. Meanwhile, by comparing Fig. 8 and Fig. 9, one can see that in both systems for a complete oscillation around the equilibrium point there is for sub-harmonies. However, for the closed-loop system based on AFSMC controller number of the intersections increases as times goes on. This is maybe because of the fact that the nonlinear and non-autonomous terms become more powerful compared to the other terms. Another observation is that the controlled system tends to vibrate in negative amplitude. This shows that the adaptive system does not suppress the vibrations symmetrically.

Figure 10 shows the phase plane diagram of the smart plate under different initial conditions. As one can see the nonlinear system has various dynamical behaviors for different initial conditions. Fig 10a depicts the system response for $\dot{x}_1(0) = 0.01, x_1(0) = 0.001, \dot{x}_2(0) = 0.001, x_2(0) = 0.01$ initial condition. It can be seen that the closed-loop system acts as a stable focus around its equilibrium point. The second case initial condition, $\dot{x}_1(0) = \dot{x}_2(0) = 0.01, x_1(0) = x_2(0) = 0.001$, acts as stable node as shown in Fig. 10b. Moreover, in the third initial condition $\dot{x}_1(0) = 0.001, x_1(0) = 0.01, \dot{x}_2(0) = 0.01, x_2(0) = 0.001$, the system phase plane shows stable focus around it's equilibrium point (see Fig. 10c). For the fourth and fifth case where the initial conditions are $\dot{x}_1(0) = \dot{x}_2(0) = 0.001, x_1(0) = x_2(0) = 0.01$ and $\dot{x}_1(0) = \dot{x}_2(0) = x_1(0) = x_2(0) = 0.001$ as depicted in Fig. 10d and Fig. 10e the closed-loop system responses in close to a saddle point.

$\dot{x}_1(0) = 0.01, x_1(0) = 0.001, \dot{x}_2(0) = 0.001, x_2(0) = 0.01$

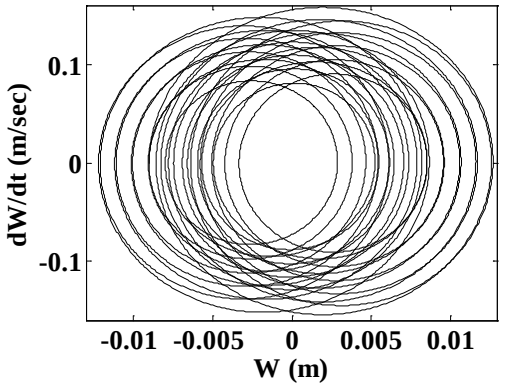

(a)

$\dot{x}_1(0) = \dot{x}_2(0) = 0.01, x_1(0) = x_2(0) = 0.001$

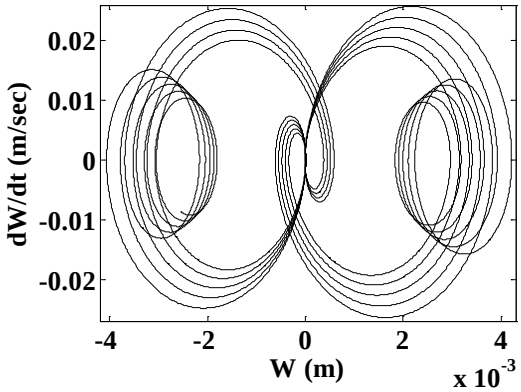

(b)

$\dot{x}_1(0) = 0.001, x_1(0) = 0.01, \dot{x}_2(0) = 0.01, x_2(0) = 0.001$

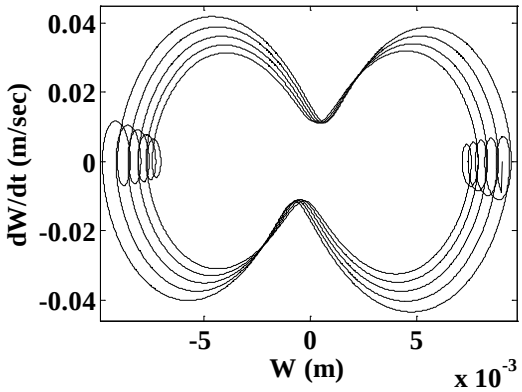

(c)

$\dot{x}_1(0) = \dot{x}_2(0) = 0.001, x_1(0) = x_2(0) = 0.01$

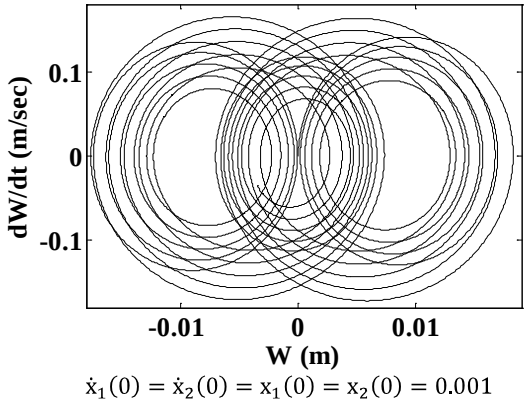

(d)

$\dot{x}_1(0) = \dot{x}_2(0) = x_1(0) = x_2(0) = 0.001$

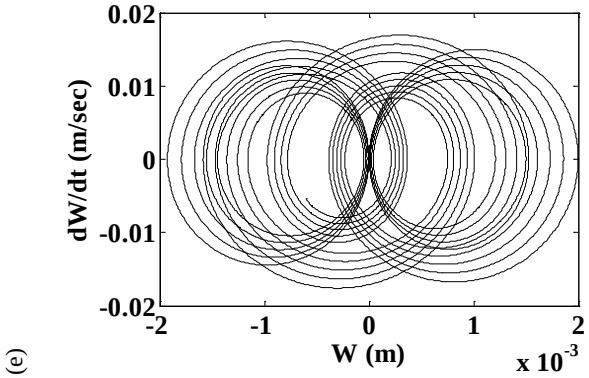

Fig. 10 Phase plane diagram of the plate under different initial conditions

V. Conclusion

Numerical investigations of a robust types of adaptive controller applied to a nonlinear plate model have been studied in this paper. Adaptive fuzzy sliding-mode control (AFSMC) is presented for the proposed nonlinear dynamic system. This controller uses the universal approximation potential of fuzzy logic control systems, accompanied by the robustness of SMCs. The parameters of the AFSMC system, together with the bound of the uncertainties are adaptively adjusted. The adaptive laws are achieved utilizing the Lyapunov stability theorem to guarantee the stability of the closed-loop system. The simulation results for the close-loop system showed that AFSMC controller is effectual for the considered plant. For higher amplitudes of excitation and random vibration, when plant's nonlinear terms play more important role, a dangerous controller's overload may appears, in the closed-loop system. It is particularly important in physical systems where maximum voltage of piezo-actuators and amplifiers is limited. The results also show that the robustness of the AFSMC scheme to plant uncertainties and external disturbances is quite promising. Finally, the closed-loop system's behaviors for different initial conditions are compared and as it has been shown in the results, the nonlinear system remains stable.

References

[1] G. C. Kung, and Y. -H. Pao, "Nonlinear flexural vibrations of a clamped circular plate," *Trans. ASME, J. Appl. Mech.*, vol. 39, pp. 1050–1054, 1972.

[2] S. D. Kisliakov, "On the nonlinear dynamic stability problem for thin elastic plates," *Int. J. Non-lin. Mech.*, vol. 11, pp. 219–228, 1970.

[3] H. Pasic, and G. Herrmann, "Effect of in-plane inertia on buckling of imperfect plates with large deformations," *J. Sound Vib.*, vol. 95, issue 4, pp. 469–478, 1984.

[4] S. Sridhar, D. T. Mook, and A. H. Nayfeh, "Non-linear resonances in the forced responses of plates, part 1: Symmetric responses of circular plates," *J. Sound Vib.*, vol. 41, issue 3, pp. 359–373, 1975.

[5] S. Sridhar, D. T. Mook, and A. H. Nayfeh, "Non-linear resonances in the forced responses of plates, part II: Asymmetric responses of circular plates," *J. Sound Vib.*, vol. 59, issue 2, pp. 159–170, 1978.

[6] X. L. Yang, and P. R. Sethna, "Non-linear phenomena in forced vibrations of a nearly square plate: Antisymmetric case," *J. Sound Vib.*, vol. 155, issue 3, pp. 413–441, 1992.

[7] A. Oveisi, M. Gudarzi, M. M. Mohammadi, and A. Doosthoseini, "Modeling, identification and active vibration control of a funnel-shaped structure used in MRI throat,", *J. Vibroeng.*, vol. 15, issue 1, pp. 438–449, 2013.

[8] J. Shan, H. Liu, and D. Sun, "Slewing and vibration control of a single-link flexible manipulator by positive position feedback (PPF)," *Mechatronics*, vol. 15, pp. 487–503, 2005.

[9] M. K. Kwak, and S. Heo, "Active vibration control of smart grid structure by multi-input and multi-output positive position feedback controller," *J. Sound Vib.*, vol. 304, pp. 230–45, 2007.

[10] M. Gudarzi, A. Oveisi, and M.M. Mohammadi, "Robust active vibration control of a rectangular piezoelectric laminate flexible thin plate: An LMI-based approach," *International Review of Mechanical Engineering*, vol. 6, no. 6, pp. 1217–1227, 2012.

[11] S. S. Oueini, A. H. Nayfeh, and J. R. Pratt, "A nonlinear vibration absorber for flexible structures," *Nonlinear Dynam.*, vol. 15, pp. 259–282, 1998.

[12] P. F. Pai, B. Wen, A. S. Naser, and M. J. Schulz, "Structural vibration control using PZT patches and non-linear phenomena," *J. Sound Vib.*, vol. 215, no. 2, pp. 273–296, 1998.

[13] S. Saguranrum, D. L. Kunz, and H. M. Omar, "Numerical simulations of cantilever beam response with saturation control and full modal coupling," *Comput. Struct.*, vol. 81, pp. 1499–1510, 2003.

[14] S. M. Hashemi-Dehkordi, M. Mailah, and A. R. Abu Bakar, "Intelligent active force control with piezoelectric actuators to reduce friction induced vibration due to negative damping," *International Review of Electrical Engineering*, vol. 4, no. 6, pp. 1294–1305, 2009.

[15] A. Karaarslan, "Obtaining renewable energy from piezoelectric ceramics using Sheppard-Taylor converter," International Review of Electrical Engineering, vol. 7, no. 2, pp. 3949–3956, 2012.

[16] S. S. Oueini, and A. H. Nayfeh, "Single-mode control of a cantilever beam under principal parametric excitation," *J. Sound Vib.*, vol. 224, no. 1, pp. 33–47, 1999.

[17] H. A. Sodano, G. Park, and D. J. Inman, "An investigation into the performance of macro-fiber composites for sensing and structural vibration applications," *Mech. Syst. Signal. Pr.*, vol. 18, pp. 683–697, 2004.

[18] L. Jun, H. Hongxing, and S. Rongying, "Saturation-based active absorber for a non-linear plant to a principal external excitation," *Mech. Syst. Signal. Pr.*, vol. 21, pp. 1489–1498, 2007.

[19] E. Ott, C. Grebogi, and J. A. Yorke, "Controlling Chaos," Physical Review Letters, vol. 64, pp. 1196–1199, 1990.

[20] K. Pyragas, "Continuous control of chaos by self-controlling feedback," *Phys. Lett. A*, vol. 170, pp. 421–428, 1992.

[21] G. Chen, and X. Dong, "On feedback control of chaotic continuous-time systems," *IEEE T. Circuits-I*, vol. 40, pp. 591–600, 1993.

[22] W. C. Y. Yang, and L. Chua, "On adaptive synchronization and control of nonlinear dynamic systems," *Int. J. Bifurcat. Chaos*, vol. 6, pp. 455–471, 1996.

[23] T. H. Yang, S. F. Chen, and Y. S. Gou, "Efficient strategy for the occasional proportional feedback method in controlling chaos," *Phys. Rev. E*, vol. 59, pp. 5393–5399, 1999.

[24] C. C. Fuh, and H. H. Tsai, "Control of discrete-time chaotic systems via feedback linearization," *Chaos Soliton. Fract.*, vol. 13, pp. 285–294, 2002.

[25] K. Konishi, M. Hirai, and H. Kokame, "Sliding mode control for a class of chaotic systems," *Phys. Lett. A*, vol. 245, pp. 511–517, 1998.

[26] H. T. Yau, C. K. Chen, and C. L. Chen, "Sliding mode control of chaotic systems with uncertainties," *Int. J. Bifurcat. Chaos*, vol. 10, pp. 1139–1147, 2000.

[27] J. M. Nazzal, and A. N. Natsheh, "Chaos control using sliding-mode theory," *Chaos Soliton. Fract.*, vol. 33, pp. 695–702, 2007.

[28] S. Bowong, and F. M. Moukam-Kakmeni, "Synchronization of uncertain chaotic systems via backstepping approach," *Chaos Soliton. Fract.*, vol. 21, pp. 1093–1108, 2004.

[29] M. T. Yassen, "Controlling, synchronization and tracking chaotic Liu system using active backstepping design," *Phys. Lett. A*, vol. 360, pp. 582–587, 2007.

[30] T. Yang, C. M. Yang, and L. B. Yang, "A detailed study of adaptive control of chaotic systems with unknown parameters," *Dynam. Control*, vol. 8, pp. 255–267, 1998.

[31] Y. J. Cao, "A nonlinear adaptive approach to controlling chaotic oscillators," *Phys. Lett. A*, vol. 270, pp. 171–176, 2000.

[32] O. Calvo, and J. H. E. Cartwright, "Fuzzy control of chaos," *Int. J. Bifurcat. Chaos*, vol. 8, pp. 1743–1747, 1998.

[33] L. Chen, G. Chen, and Y. W. Lee, "Fuzzy modeling and adaptive control of uncertain chaotic systems," Information Sciences, vol. 121, pp. 27–37, 1999.

[34] Y-C. Chang, "A robust tracking control for chaotic Chua's circuits via fuzzy approach," *IEEE T. Circuits-I*, vol. 48, pp. 888–895, 2001.
[35] C. W. Park, C. H. Lee, and M. Park, "Design of an adaptive fuzzy model based controller for chaotic dynamics in Lorenz systems with uncertainty," *Inform. Sciences*, vol. 147, pp. 245–266, 2002.
[36] X. Guan, and C. Chen, " Adaptive fuzzy control for chaotic systems with tracking performance," *Fuzzy Set. Syst.*, vol. 139, pp. 81–93, 2003.
[37] O. V. Ramana Murthy, R. K. P. Bhatt, and N. Ahmad, "Extended dynamic fuzzy logic system (DFLS) based indirect stable adaptive control of non-linear systems," *Appl. Soft Comput.*, vol. 4, pp. 109–119, 2004.
[38] J. H. Kim, C. W. Park, E. Kim, and M. Park, "Fuzzy adaptive synchronization of uncertain chaotic systems," *Phys. Lett. A*, vol. 334, pp. 295–305, 2005.
[39] L. X. Wang, "Adaptive Fuzzy Systems and Control: Design and Stability Analysis," Prentice-Hall, New Jersey, 1994.
[40] H. Chu, and G. Herrmann, "Influence of large amplitudes in free flexural vibrations of rectangular elastic plates," *J. appl. Mech.*, vol. 23, pp. 532-540, 1956.
[41] A. Y. T. Leung, and S. K. Chui, "On the non-linear vibration of the Von Karman square plate by the IHB method," *J. Sound Vib.*, vol. 204, issue 2, pp. 239-247, 1997.
[42] J. -J. E. Slotine, and W. Li, "Applied Nonlinear Control," Prentice-Hall, New Jersey, 1991.
[43] H. Khalil, "Nonlinear Systems," Prentice Hall, New Jersey, 1996.
[44] C. M. Lin, and C.F. Hsu, "Self-learning fuzzy sliding mode control for antilock braking systems," *IEEE T. Contr. Syst. T.*, vol. 11, pp. 273–278, 2003.